nature portfolio

https://doi.org/10.1038/s41596-023-00803-0

Supplementary information

Quantitative multiple fragment monitoring with enhanced in-source fragmentation/ annotation mass spectrometry

In the format provided by the authors and unedited

SUPPLEMENTARY MATERIAL

Quantitative Multiple Fragment Monitoring with Enhanced In-Source Fragmentation/Annotation Mass Spectrometry

Samuel Bernardo-Bermejo[a,*], Jingchuan Xue[b,*], Linh Hoang[c], Elizabeth Billings[c], Bill Webb[c], M. Willy Honders[d], Sanne Venneker[e], Bram Heijs[f], María Castro-Puyana[a], María Luisa Marina[a], Erik B. van den Akker[g,h,i], Marieke Griffioen[d], Gary Siuzdak[c,#], Martin Giera[f,#], and Elena Sánchez-López[f,#]

[a] Universidad de Alcalá, Departamento de Química Analítica, Química Física e Ingeniería Química, Ctra. Madrid-Barcelona Km.33.600, 28871 Alcalá de Henares (Madrid), Spain.

[b] Guangdong Provincial Key Laboratory of Water Quality Improvement and Ecological Restoration for Watersheds, Institute of Environmental and Ecological Engineering, Guangdong University of Technology, Guangzhou, 510006, China.

[c] Scripps Center for Metabolomics, The Scripps Research Institute, 10550 North Torrey Pines Road, La Jolla, California 92037, United States.

[d] Department of Hematology, Leiden University Medical Center, 2300RC, Leiden, The Netherlands.

[e] Department of Pathology, Leiden University Medical Center, Leiden, 2300RC, The Netherlands

[f] Center for Proteomics and Metabolomics, Leiden University Medical Center, 2300RC Leiden, Netherlands.

[g] Center for Computational Biology, Leiden University Medical Center, 2300RC, Leiden, The Netherlands.

[h] The Delft Bioinformatics Lab, Delft University of Technology, 2628CD, Delft, The Netherlands.

[i] Section of Molecular Epidemiology, Leiden University Medical Center, 2300RC, Leiden, The Netherlands.

*Shared co-first authorship.

[#]Corresponding authors:

Gary Siuzdak. Scripps Center for Metabolomics, The Scripps Research Institute, 10550 North Torrey Pines Road, La Jolla, California 92037, United States. siuzdak@scripps.edu

Martin Giera and Elena Sánchez-López. Center for Proteomics and Metabolomics, Leiden University Medical Center, 2300RC Leiden, Netherlands. m.a.giera@lumc.nl and E.Sanchez_Lopez@lumc.nl

Table of contents:

Procedure section

Optimization of the LC conditions. To carry out the separation of the diastereomers of DL-2-HG upon derivatization with L-DATAN, three different columns were compared (C18 column (100 x 2.1 mm; 1.7 µm), Aqua C18 column (100 x 2 mm; 2.5 µm) and Aqua C30 column (150 x 2 mm; 3 µm)). The mobile phases were mobile phase A (3.5% (v/v) acetonitrile:water) + 125 mg/L ammonium formate, pH 3.6) and mobile phase B (50% (v/v) acetonitrile:water). Taking into account the peak shape and the resolution achieved, the Aqua C30 column was selected (**Figure S1**). Given their somewhat polar nature, DATAN-2-HG diastereoisomers had very low retention on the assessed columns, thus, we evaluated the retention with a mobile phase A containing solely water with 125 mg/L ammonium formate pH 3.6 (no acetonitrile present). The mobile phase without acetonitrile improved the resolution (**Figure S2**). Increasing or lowering the pH to 5.0 or 2.6, respectively, did not improve the separation as can be seen in **Figure S3**. Keeping in mind the intended application of the method to the analyses of biological samples, we aimed to increase the amount of organic solvent in the mobile phase B up to 95% in order to guarantee a proper cleaning of the chromatographic column after each run. As expected, under the same gradient conditions, increasing the ACN concentration resulted in a decreased resolution so the gradient was modified accordingly to account for this decrease (**Figure S4**). Finally, the injection volume was tested from 10 to 40 µL, where 20 µL was the highest possible volume that did increase the sensitivity without severely harming the separation (data not shown).

The rest of the chromatographic parameters and the gradient employed were:

- Flow rate: 0.4 mL/min.
- Oven temperature: 22 ºC.

Gradient :

- 0% B: 0.0 min.
- 0% B to 36% B: 5.0 min.

- 36% B to 100% B: 6.0 min.
- 100% B: 8.0 min.
- 100% B to 0% B: 8.4 min.
- 0% B: 13.0 min.

Note that in this particular case the optimization of the chromatographical parameters was carried out using MS/MS (hence the low number of points per peak on **Figures S1-S4**. However, this is not mandatory and users can still carry out the optimization using a single mass analyzer.

EISA optimization. Once the optimum conditions for the chromatographic separation were selected, the different parameters that enhance an in-source fragmentation were studied, namely end plate offset, capillary voltage, nebulizer pressure, drying gas and in-source collision induced dissociation (isCID). The aim was to obtain both the precursor ion and the corresponding fragment of DL-2-HG to selectively establish an in-source fragmentation relation. In this way, the identification and quantification of this compound can be carried out through a single run in full scan mode without the need for MS/MS instrumentation.

Following our procedure detailed in **Box 1**, a 2.5 mM solution of the derivatized DL-2-HG was directly infused into the ESI source and the highest intensity of both the fragment *m/z* 147.0270 and the precursor ion *m/z* 363.0570 was the criterion followed to select the best conditions. End plate offset was the first parameter studied from 0 to 2000 V where 10 V showed the highest intensity (**Figure 3a**). Then, in order to further enhance the in-source fragmentation, capillary voltages from 3000 to 5000 V were evaluated. However, the precursor ion was not found for values lower than 4000 V being this voltage the one with the highest intensity of both ions (**Figure 3b**). Different nebulizer pressure from 1.0 to 2.4 bar were assessed and 1.6 bar was the one selected due to the fact that it had the highest intensity (**Figure 3c**). The next parameter optimized was the N_2 dry gas flow (1-10 L/min), which aids desolvating in the electrospray source. Although the

highest intensity obtained was using 1 L/min (**Figure 3d**), the ion signal was not stable at such low flow so we chose 6 L/min which still displayed a high intensity maintaining a stable ion signal.

Lastly, the isCID voltage was assayed. Some metabolites might still need an extra help to enhance their in-source fragmentation, where increasing the isCID may be of relevance. Since we wanted to investigate whether it had an effect in the signal-to-noise ratio (S/N) per enantiomer we assessed this using the chromatographic method, instead of via direct infusion. 0, 10 and 20 eV resulted in very similar S/N (**Figure 4**) so, for simplicity, 0 eV was eventually selected. Note that values higher than 40 eV resulted in the complete fragmentation of the precursor ion. If more than one product ion is obtained, under optimum LC-MS conditions evaluate what combination of precursor + product/s ions gives the highest signal-to-noise ratio (S/N). In our case, the precursor (*m/z* 363.0570) + just one product (*m/z* 147.0270) ion gave the best S/N.

To conclude, the optimized conditions were:

- End Plate Offset: 10 V.
- Capillary: 4000 V.
- Nebulizer: 1.6 bar.
- Dry Gas: 6 L/min.
- Transfer isCID Energy: 0 eV.
- Extracted Ion Chromatogram: *m/z* 363.0570 + 147.0270.

The rest of MS-related parameters are included below:

- Dry Temp: 350 ºC.

Transfer:

- Funnel 1 RF: 200.0 Vpp.
- Funnel 2 RF: 300.0 Vpp.

- Hexapole RF: 100.0 Vpp.

Quadrupole:

- Ion Energy: 5.0 eV.
- Low Mass: *m/z* 80.00.

Collision Cell:

- Collision Energy: 0.0 eV.
- Collision RF: 300.0 Vpp.
- Transfer Time: 80 µs.
- Pre Pulse Storage: 4.0 µs.

Supplementary Figures

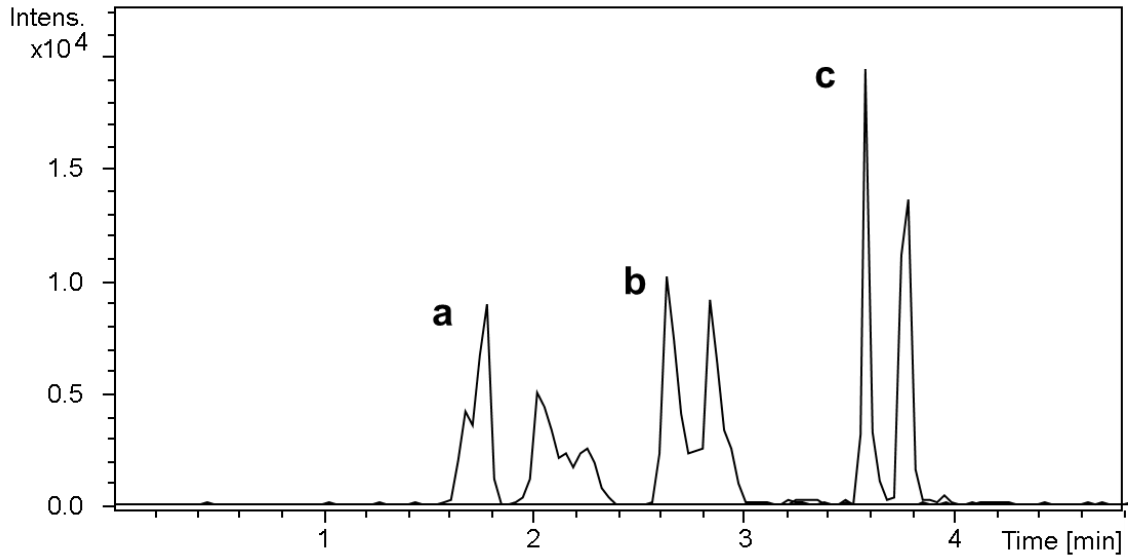

Figure S1. Extracted ion chromatograms of the DL-2-HG separation by the three different columns evaluated: (a) C18 column (100 x 2.1 mm; 1.7 µm); (b) Aqua C18 column (100 x 2 mm; 2.5 µm); (c) Aqua C30 column (150 x 2 mm; 3 µm). In all cases L-2-HG was the first eluting peak, while D-2-HG was the second (concentration of 20 µmol/L per enantiomer). Chromatographic traces were extracted using the *m/z* 363 → 147 MS/MS transition with a *m/z* ± 0.1.

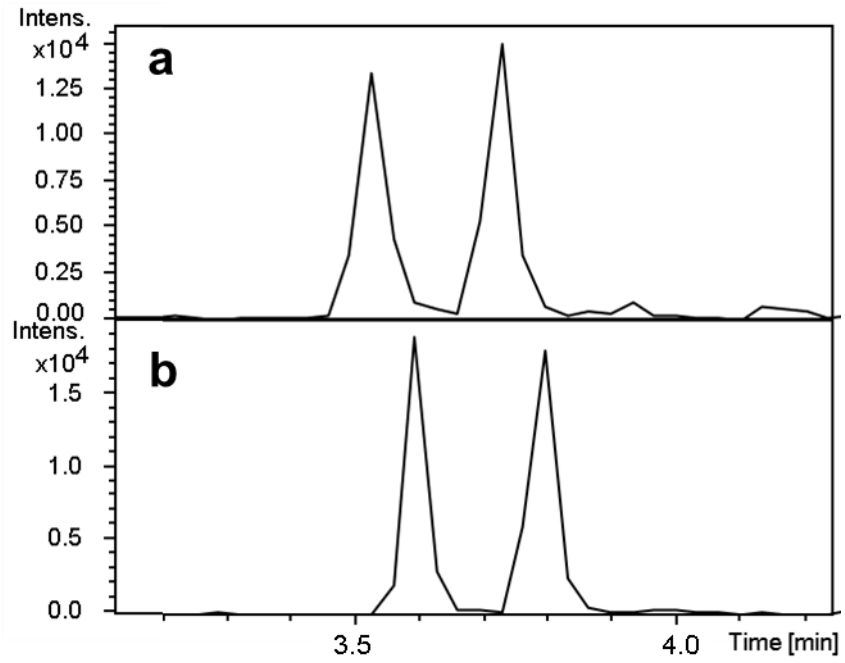

Figure S2. Extracted ion chromatograms of the DL-2-HG separation investigating the effect of the presence (a) or absence (b) of ACN in the mobile phase A: (a) 3.5% (vol/vol) acetonitrile:water + 125 mg/L ammonium formate (pH 3.6); (b) 125 mg/L ammonium formate in water (pH 3.6). In both cases L-2-HG was the first eluting peak, while D-2-HG was the second (concentration of 20 µmol/L per enantiomer). Chromatographic traces were extracted using the *m/z* 363 → 147 MS/MS transition with a *m/z* ± 0.1.

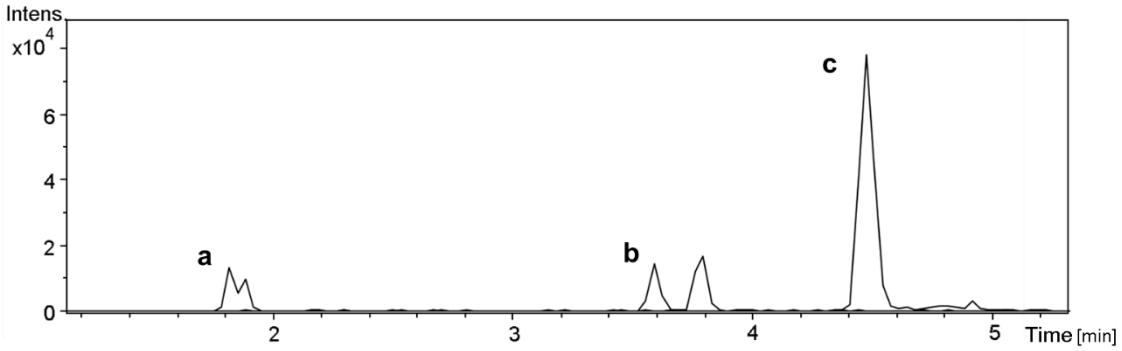

Figure S3. Overlapped extracted ion chromatograms of the DL-2-HG separation investigating the effect of different pH in the mobile phase A: (a) 125 mg/L ammonium Acetate in water (pH 5.0); (b) 125 mg/L ammonium formate in water (pH 3.6); (c) 0.1% (v/v) formic acid:water (pH 2.6). In all cases L-2-HG was the first eluting peak, while D-2-HG was the second (concentration of 20 µmol/L per enantiomer), except on c where no resolution was achieved. Chromatographic traces were extracted using the *m/z* 363 → 147 MS/MS transition with a *m/z* ± 0.1.

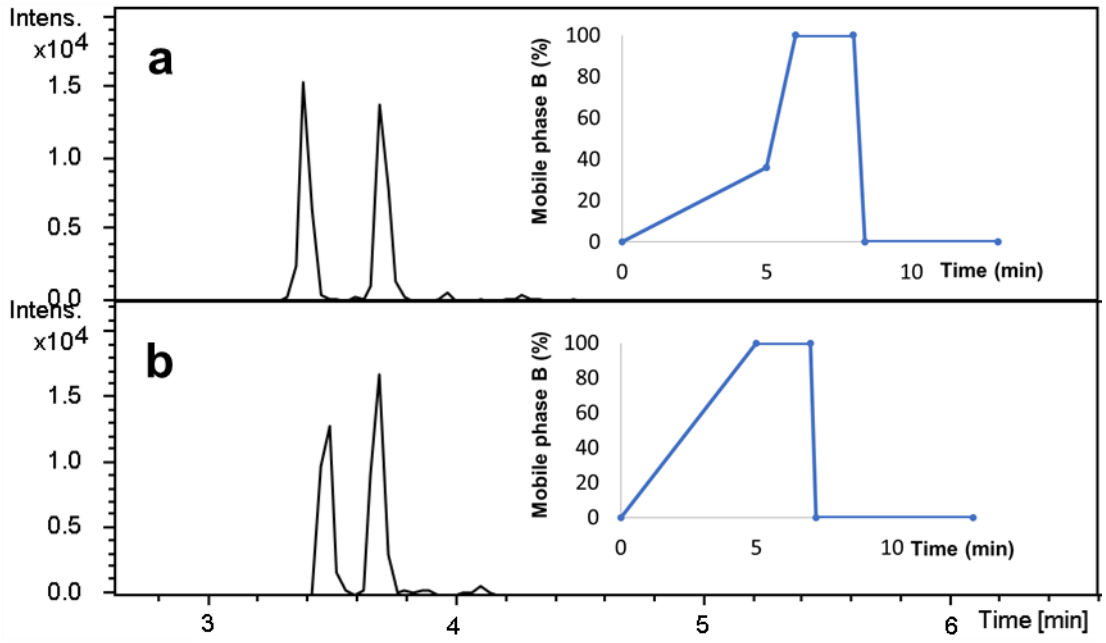

Figure S4. Extracted ion chromatograms of the DL-2-HG separation investigating the effect of the concentration of acetonitrile in the mobile phase B: (a) 95% (v/v) acetonitrile:water (b) 50% (v/v) acetonitrile:water. The chromatographic gradient used for each condition is included on the right of each panel. In both cases L-2-HG was the first eluting peak, while D-2-HG was the second (concentration of 20 µmol/L per enantiomer). Chromatographic traces were extracted using the *m/z* 363 → 147 MS/MS transition with a *m/z* ± 0.1.

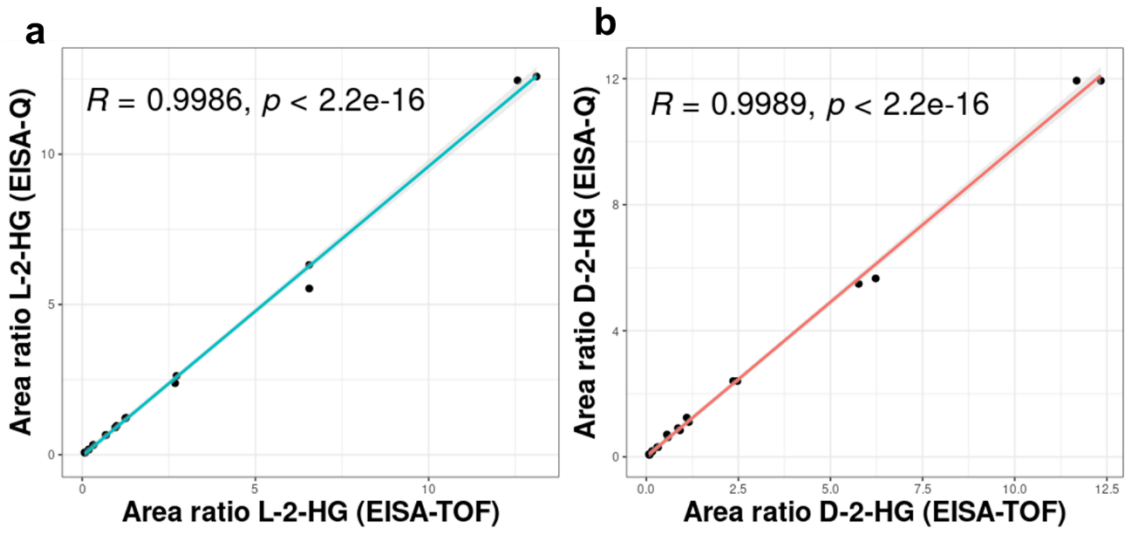

Figure S5. Correlation plots between the area ratios found for (a) L-2-HG and (b) D-2-HG corrected by the area of the internal standard (L- and D-2-HG-d_3, respectively), in the calibration line (0.5–100 µmol/L) analyzed by EISA-Q and EISA-TOF. R and p-values for Pearson correlation are given in each panel. For details on all concentrations used in the calibration lines see **Table 1**.